Combined Impact of Carbonation and Crack Width on the Chloride Penetration and Corrosion Resistance of Concrete Structures

Abbas S. AL-Ameeri [1,2], M. Imran Rafiq[1] and Ourania Tsioulou [1]

[1] School of Environment and Technology, University of Brighton, Brighton, UK

[2] Engineering College, University of Babylon, Babylon, Iraq

Abstract. Chloride-induced corrosion of steel rebar embedded in concrete is one of the major concerns influencing the durability of reinforced concrete structures. It is widely recognized that the carbonation in concrete affects the chloride diffusivity and accelerates chloride-induced reinforcement corrosion. The service load related cracks also have a dominant influence on the reinforcement corrosion. This study aims to investigate the potential impact of concrete carbonation on the chloride penetration resistance, and the rate of corrosion, in RC structures subjected to service related cracks, which is not yet fully understood within the literature. The experimental programme involves casting concrete prisms (100 x 100 x 500 mm) with different water-cement ratios of 0.4, 0.5 and 0.6 and with four different crack width ranges (0, 0.05-0.15 mm, 0.15-0.25 mm and 0.25-0.35 mm), developed through flexural loading of prisms. These samples were exposed initially to accelerated carbon dioxide (CO_2) environment and then exposed to the accelerated chloride environment. Carbonation depth, chloride penetration, and the degree of corrosion (using half-cell potential and linear polarization resistance) were experimentally measured. The results indicated that (i): The depth of carbonation increases with the increase in crack width and w/c ratio, (ii) chloride penetration depth and chloride concentration profile in concrete structures increases significantly due to the influence of carbonation and (iii) half-cell corrosion potential and linear polarization resistance increases significantly when carbonated concrete samples are exposed to the chloride environment relative to the uncarbonated concrete samples.

1 Introduction

Carbon dioxide and chloride ions attack are known to significantly affect the durability of concrete structures. Furthermore, exposure environment such as the temperature and relative humidity also affect the penetration of chloride and sulfate in the concrete structures. As a result, the diffusivity of carbon dioxide and chloride have a significant impact on corrosion in concrete structures (Neville, 2011, Hussain et al., 1995) [1, 2]. Temperature, relative humidity and carbonation have considerable impact on penetrability of chloride (from external sources) and activation of chloride (from internal sources) within the concrete. De-icing salt, seawater and groundwater are examples of the chloride from external

sources, whereas the internal sources of chloride may be attributed to the chemical composition of concrete components (aggregate, cement and water) such as marine aggregate and chemical admixtures containing chloride ions (Dyer, 2014) [3].

The composition of cement, in particular tri-calcium aluminate (C_3A), slows down the chloride ions penetration rate by binding the chloride ions into calcium chloroaluminate (Friedel's salt) (Neville, 2011, Dyer, 2014) [1, 3]. The carbonation in concrete leads to changes in the mineralogical composition of concrete and reduces the pH of pore water in concrete (Broomfield, 2007) [4]. It has the potential to also liberate the bound chloride ions, which potentially increases the chloride ions concentration leading to its deeper chloride penetration into the concrete (Wan et al., 2013) [5]. The carbonation of cement paste achieves in a release of bound chlorides, which is regarded to not only the decomposition of Friedel's salt (calcium chloroaluminate), but also the decomposition of calcium-silicate-hydrate (C-S-H) gel (Geng, et al. 2016, Shen, et al. 2019) [6,7].

Cracks in concrete structures are expected due to its weak tensile strength. Cracks can be either non-structural or structural. Structural cracks tend to be wider (> 0.1 mm) while non-structural cracks are generally finer. Structural cracks often result from one, or a combination, of the following reasons: insufficient reinforcement, low strength of concrete, excessive loading magnitude or frequency, impact loading, permanent actions such as foundation settlement, creep, etc. While, the non-structural cracks may occur due to physical impact (shrinkable aggregate, drying shrinkage), chemical effect (carbonation shrinkage and alkali -silica reaction) and thermal impact (expansion/contraction due to external temperature variation and freeze and thaw cycle) (ACI224.R-01 & TR22) [8,9]. The cracks may also be the result of deterioration and loss of durability of material or are worsened due to the degradation of material. The durability of concrete structures is controlled by their capacity to delay the transport of ions and harmful fluids inside the concrete. The transport of chloride within uncracked concrete is said to be a combination of the concentration gradient (diffusion), the pressure gradient (permeation) and capillary sorption (Dyer, 2014, Morcous and Lounis, 2005) [3, 10]. The cracks in concrete introduce an additional factor within the transport properties of concrete, namely the permeability of concrete, which is likely to significantly increase the transport of chloride ions inside concrete (Shao-feng et al., 2011) [11]. Park et al.(2012)[12] found the chloride diffusion coefficient in concrete increases 24 times for crack width of 0.1 mm and 145 times for crack width of 0.4 mm, when compared with the un-cracked concrete. These results are not fully in agreement with the results obtained in (Shao-feng et at.,2011, Kwon et al., 2009) [11, 13] due to natural formation of cracks in the sample (width, depth and tortuosity) or the method of assessing the diffusion coefficient of chloride.

The studies of durability assessment in literature, such as corrosion initiation, often excludes the effect of carbonation and cracks, voids and defects in concrete, thereby their effectiveness in predicting the durability of concrete structures is reduced (Kwon et al., 2009) [13]. Therefore, it is important to investigate the influence of carbonation and service cracks

on the penetration of chloride and the degree of corrosion. Moreover, carbonation and chloride negatively affect the passive protective film (PPF) of steel reinforcement in concrete structures (Neville, 2011) [1], which accelerates the corrosion of reinforced concrete structures (Neville and Brooks, 1987, Dyer, 2014) [3, 14]. The focus of this study is to examine and investigate the impact of carbonation in reinforced concrete samples on the penetration of chloride, chloride concentration profile and rate of corrosion in cracked and un-cracked concrete samples.

2 Experimental work

2.1 Materials and concrete Mix Design

Portland limestone cement (CEM II/A-LL 32,5R) with a specific gravity of 3.05 was used in this study. Chemical and physical properties of the cement comply with BS EN 197- 1: 2011 [15].

Natural sand was used as fine aggregate (particle size < 5mm), and the coarse aggregate used was crushed gravel with the size ranging from 5-14 mm. The grain size distribution, and maximum chloride and sulphate content within the aggregates comply with BS 882:1983 [16]. Deformed or ribbed steel (B500A) (8mm) with mechanical properties which are compliant with BS 4449:2005+A2:2009 [17] was used to reinforce the concrete prisms to achieve the controlled crack widths in the samples, and to investigate the corrosion condition.

Three different w/c ratios were used to investigate their effects on the carbonation and chloride penetration depth .The Building Research Establishment (BRE) method [18] was used for design of the concrete mixes as shown in Table 1.

Table 1 Concrete mixes design according to the method of Building Research Establishment (1988) [18]

Mix symbol	Content per unit volume of concrete (kg / m^3)				
	w/c	Cement	Water	Sand	Gravel
M 0.4	0.4	513	205	653	980
M 0.5	0.5	410	205	711	1023
M 0.6	0.6	350	205	711	1041

2.2 Specimen Geometry

Three 100 mm cube specimens were used for testing the compressive strength and porosity of concrete. Three reinforced concrete prisms of 100 x 100 x 500 mm were used to measure the depth of carbonation (DoC), chloride penetration and corrosion condition (using half-cell corrosion potential) in both the cracked and un-cracked specimens. A deformed steel bar (B500A) of 8mm diameter was located at a cover depth of 20 mm to reinforce the concrete prisms to achieve the controlled crack sizes within the samples and to investigate the half-cell corrosion potential and linear polarization

resistance. The method of preparation of moulds, casting, compaction and levelling the surface of concrete, curing and transporting of samples were in accordance with BS EN 12390 -2:2009 [19]. Samples were cast in two layers and each layer was vibrated to achieve homogenous concrete. The specimens were demoulded and cured using tap water until the time of testing, or exposure to CO_2 or chloride environmental conditions at the age of 28 days.

2.3 Specimens Conditioning

Flexural method (three point bending) was used to induce the required crack widths within the concrete samples as shown in Fig.1. In addition to the un-cracked samples, three different crack width ranges, (0.05-0.15mm, 0.15-0.25mm and 0.25-0.35mm) were examined. The crack width was measured using a microscope meter with an accuracy of 0.01 mm (Fig. 2). . The crack widths were measured in the samples after unloading (once the load was removed from frame of loading). The crack depth, D_{crack} , was computed by measuring the time of transfer of pulse velocity using the ultrasonic device according to the Equation 1 [20] . Fig. 3 is illustrated the methods for crack depth measurement. The reinforcement steel bar can control on crack width and depth in concrete sample.

$$D_{crak} = x\sqrt{\frac{T_c^2}{T_s^2} - 1} \qquad (1)$$

where:

2x is the path length without crack; Tcr is travel time around the crack and Ts is surface travel time through sound concrete without a crack (2x).

The crack depths are ranging 15-25 mm, 25-35 mm and 35-40 mm for 0.05-0.15mm, 0.155-0.25mm and 0.255-0.35 mm respectively.

In this study, one face of the specimens was exposed to accelerated environment conditions whereas the other faces were sealed (using multiple coats of water-based alkyl polysiloxane resin).

The control samples were exposed to a chloride fog environment (with 5% NaCl) within a Cyclic Chloride Test (CCT) chamber for 15 weeks in total. The rest of the samples were taken out of the CCT chamber after 10 weeks of chloride exposure and were exposed to CO_2 concentration of 5% within a CO_2 chamber (at a temperature of 25 ºC and relative humidity of 65%) for 5 weeks before returning them back in the CCT chamber (chloride exposure) for the remaining 5 weeks.

Fig. 1. Flexural method was used to create the crack in concrete sample

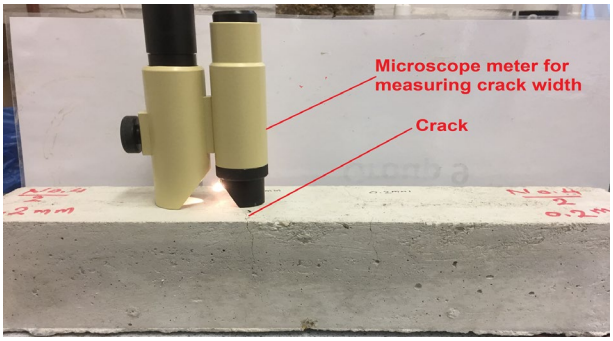

Fig.2. Microscope meter used to measure the cracks width

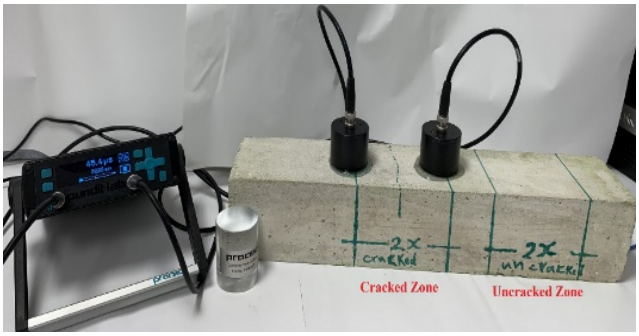

Fig. 3*:* Measuring the crack depth by pulse velocity of the ultrasonic devices

2.4 Testing Methodologies

The compressive strength, ultra-sonic pulse velocity, porosity, depth of carbonation (DoC), chloride penetration, and half-cell potential were carried out for this study. Porosity and compressive strength test were conducted according to ASTM C642:2013 [21] and BS EN 12390-3:2000 [22] respectively. The chloride penetration depth and chloride concentration profile were measured by splitting the conditioned samples into two parts (using a compression testing machine). The first part was sprayed with 0.1% silver nitrate solution in accordance with (Yuan et al., 2008, He et al., 2011) [23,24]. The silver nitrate solution reacts with chloride ions to form silver chloride, changing the colour of the concrete surface hence the depth of chloride penetration can be measured [23,24]. While, the second part of the sample was drilled near the crack locations to collect a concrete powder at different depths to establish total chloride concentration profile according to BS EN 12390-11(2015) [25] using chloride titration. The concrete powder was collected from the exposed face at seven depth intervals; 0-6 mm, 6-12 mm, 12-18 mm, 18-24 mm, 24-30 mm, 30-36 mm and 36-42 mm and non-exposure sample powder, using dry drilling equipment. The concrete powder was sieved using 150 micro-meter sieves to reduce the amount of coarse grains of the aggregates. The powder was then dried in an oven at 50°C for 24 hours and kept in sealed plastic bags until tested.

The following procedure was adopted for the titration method (to measure total chloride concentration of chloride in the concrete dust samples). 1 g of the powder was dispersed in 100 ml of (distilled water and nitric acid) and boil for 3 minutes

to leach out the chloride ions. The solution was filtered using a fast grade filter paper and made up to 100 ml by adding distilled water. Titration was carried out with 0.1M silver nitrate. Three specimens were tested for each case and an average value is reported in the results.

In order to measure the depth of carbonation, CO_2 conditioned samples were split into two parts using the same procedure as above in accordance with Al-Amoudi et al. 1991[26]. The first part was sprayed with a phenolphthalein solution (one gram of phenolphthalein powder dissolved into a solution of 70 ml and 30 ml of ethanol and deionized water respectively) (BS EN 13295(2004), BS EN 12390-10(2018)) [27,28]. The change of colour of concrete surface was then used to determine the carbonation depth, DoC. Dry drilling method was used to collect concrete powder from the second part of the sample at different depths from the exposed surface. Seven depth intervals were adopted in this study; 0-6 mm, 6-12 mm, 12-18 mm, 18-24 mm, 24-30 mm, 30-36 mm and 36-42 mm. The collected concrete powder was then sieved using 150 micro-meter sieves to reduce the amount of coarse grains (obtained due to crushing of aggregates). The powder was then dried in an oven at 50°C for 24 hours and kept in sealed plastic bags till tested.

The apparent pH of the powder was measured by dissolving 1 g of concrete powder in 20 ml of deionized water. This mixture (powder and water) was stirred vigorously for 30 seconds and left to settle for 24 hours (McPolin et al., 2007, Wang et al., 2016) [29,30]. A pH meter was used to measure the apparent pH of this solution in accordance with BS EN ISO 10523:2012 [31]. Three specimens were tested for every case and an average value is reported in the results.

Finally, the corrosion monitoring tests were carried out using non-destructive techniques. These techniques have been utilized to assess the corrosion activity and determine the corrosion rate of the reinforcement. Two of the most used electrochemical techniques were used for monitoring the corrosion of steel in concrete, the half-cell potential and the Linear Polarization Resistance, LPR. The half-cell potential and the LPR test were performed in accordance with the ASTM C876:2015[32] and the method proposed by Bouteiller et al., (2012) [33] respectively as shown in Fig.4. Three specimens were tested for each case and the average results of these are reported in the results.

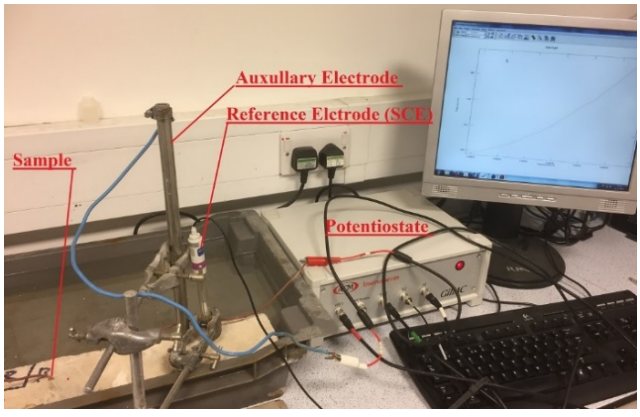

Fig. 4. Half-cell potential and Linear Polarization Resistance measurement using Potentiostat

3 Results and Discussion

In this section, the results of the experimental work are presented and discussed. These are mainly focused on the impact of carbonation on the depth of chloride penetration, chloride concentration profiles, and the corrosion rate for various w/c ratio (representing the strength of concrete) and crack width in concrete samples.

3.1 Carbonation Depth in Concrete

The depth of carbonation (DoC) at various points along the sample width was measured (Fig. 5) and an average of these measurements are presented in the results. The DoC as a function of w/c ratio for the mixes used in this study is shown in Table 2, where M 0.4, M 0.5 and M 0.6 refers to w/c ratio of 0.4, 0.5 and 0.6 respectively. The results illustrate that the carbonation depth increases significantly with the increase in w/c ratio in concrete samples.

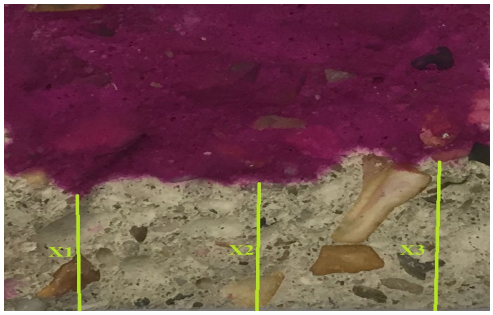

Fig.5. Typical DoC measurement in concrete samples

The percentage increases in DoC for samples having w/c ratio 0.5 and 0.6 with respect to the concrete samples with w/c ratio of 0.4 are 25% and 113% respectively.

Table 2 Depth of carbonation and concrete properties.

Property	Concrete Mixes		
	M 0.4	M 0.5	M 0.6
DoC at 5% CO_2 (mm)	8.0	10.0	17.0
Coefficient of variation (COV) of DoC	3.3	2.6	1.6
Porosity %	10.1	11.1	11.5
Compressive strength (MPa)	53.2	48.1	39.7

The increase of DoC in concrete mixes as a function of the w/c ratio is a result of the increase in porosity of concrete (also shown in Table 2) and volume of permeable voids, i.e. the pore system of the hardened cement paste (Neville, 2011, Basheer et al., 2001) [1,34], that helps CO_2 to penetrate and react with water to form carbonic acid, the latter then reacts with $Ca(OH)_2$ to form the carbonation products ($CaCO_3$) (Chi et al., 2002) [35].

Fig. 6 presents the apparent pH profile within the concrete depth, obtained using the dust powder collected at various depths within the concrete samples. The results clearly demonstrate a reduction in the apparent pH near the surface region of concrete (affected by carbonation), which is more pronounced for higher w/c ratios. The increase in w/c ratio lead to an increase the penetration of CO_2, which in turn increases the consumption of the alkalinity sources in concrete (i.e. $Ca(OH)_2$ and C-S-H) (McPolin et al., 2007, Wang et al., 2016) [29- 30], hence the pH levels reduced within the depth of concrete are affected by carbonation.

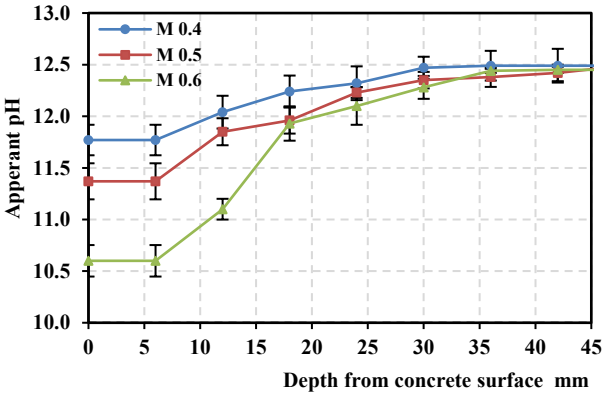

Fig. 6. Apparent pH profile in concrete due to carbonation

3.2 Chloride concentration and penetration

Two sets of concrete samples were tested for chloride penetration; the first set was exposed to a CO_2 environment in-between the exposure to the chloride fog environment, whilst the second set was just exposed to the chloride fog (control specimen). The difference between the series is the first was exposed to an accelerated CO_2 environment, while the second was exposed to a normal CO_2environment and exposure time to CO_2 for both was 5 weeks. The specimens were split longitudinally, and the freshly fractured first face sprayed with silver nitrate ($AgNO_3$). The $AgNO_3$ colourimetric method was used to measure the chloride penetration depths (d_{cl}^-) (Yuan et al., 2008, He et al., 2012) [23, 24]. The second face was drilled with depth to collect the concrete powder to measure experimentally total chloride concentration according to BS EN 12390-11(2015) [25].

3.2.1 Chloride penetration depth in concrete

The silver nitrate ($AgNO_3$) colorimetric method was used to measure penetration depths of the chloride front (d_{cl}^-). The $AgNO_3$ solution spray reacts with chloride ions to form a mixture of silver oxide and silver chloride that precipitates on the concrete surface and changes colour forming a boundary corresponding to the chloride penetration depth (Yuan et al., 2008, He et al., 2012) [23,24] within the concrete specimens. Results for the two sets for different crack widths and w/c ratio are presented in Fig. 7. Key observations from these results are:

(i) The results exhibit higher chloride penetration depths for samples exposed to CO_2 environment when compared with the uncarbonated samples as shown in Fig.7 and 8, and Table 3, particularly for the uncracked concrete samples. This can be attributed to the fact that the carbonation reduces the pH of the pore water in concrete which is a significant factor in liberation of bound chlorides (calcium chloroaluminate) in cement mortar (Wan et al., 2013) [5] hence increases free chloride concentration and ultimately the penetration depth.

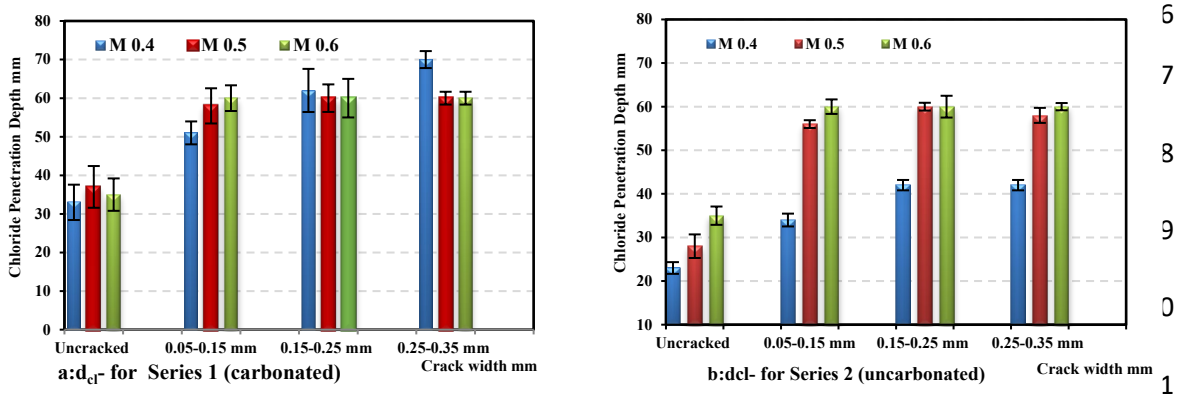

Fig.7. Effect of w/c ratio and cracked width on chloride penetration(d_{cl}-) for uncarbonated and carbonated samples

Table 3 Percentage change in chloride penetration depth (d_{cl}-) between carbonated and uncarbonated specimens

Sample	Increase percentage in chloride penetration depth (d_{cl}-) (%)			
	Un-cracked	0.05 -0.15 mm	0.15-0.25 mm	0.25-0.35 mm
M 0.4	43	50	48	67
M 0.5	32	4	0	3
M 0.6	0	0	0	0

(ii) The results depict an increase in chloride penetration with the increase in w/c ratio for both sets of concrete samples (i.e. with and without carbonation) particularly for the uncracked samples as shown Fig.8. This can be explained by the fact that the w/c ratio affects the volume of internal voids or porosity in the concrete that in turn affects the chloride ions transport mechanisms in concrete, i.e. diffusion, permeation, sorption and permeability (Basheer et al., 2001) [34]. The percentage increase in chloride penetration depth with the increase in w/c ratio are shown Table 4.

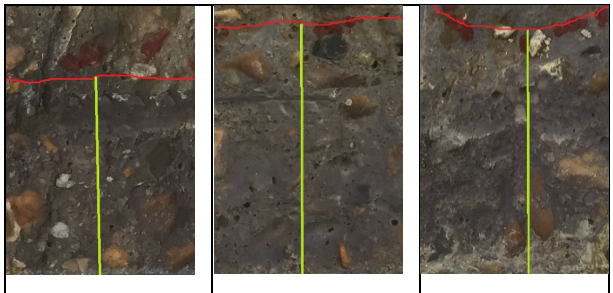

a: M 0.4	b:M 0.5	c:M 0.6

d: M 0.4	e:M 0.5	f:M 0.6

Fig. 8. Effect the w/c ratio and carbonation on d_{cl}^- for Un-cracked sample (a, b and c) carbonated-Series 1 and (d, e and f) Un-carbonated -Series2
Red line is the boundary of chloride penetration.
Yellow line is the depth of chloride penetration

Table 4 Percentage increase in chloride penetration depth for M 0.5 and M 0.6 samples with respect to M 0.4

Series	Sample	Percentage increase (%)			
		Un-cracked	0.05 -0.15 mm	0.15-0.25 mm	0.25-0.35 mm
Series 1 carbonated	M 0.5/M 0.4	12	14	-3	-14
	M 0.6/M 0.4	6	18	-3	-14
Series 2 uncarbonated	M 0.5/M 0.4	22	65	43	38
	M 0.6/M 0.4	52	76	43	43

(iii) The chloride penetration depth increases with the crack widths for the all mixes till a threshold crack width is reached, which is estimated from Fig. 7 to be around 0.1 mm. The crack width and depth affect the transport mechanism of chloride ion into the crack opening since wider cracks may allow the chloride solution to penetrate in the cracks (Audenaert et al., 2009, Suzuki et al., 1990) [36,37]. The cracks of width less than 0.1 mm appear to have contributed only through an increase in the rate of transport of chloride ions (i.e. increase in permeability and diffusion rates of concrete). However, cracks of width greater than 0.1 mm appears to have provided additional surface area (along the crack walls) for the transport of chloride ions into concrete. Hence, an increase in chloride penetration perpendicular to the crack walls can also be observed (Fig. 9), which is similar to the chloride penetration profile from the surface of an uncracked concrete. The percentage increase in chloride penetration depth for cracked samples in relation to the uncracked samples are shown in Table 5.

Table 5 Percentage increase in chloride penetration depth (d_{cl}-) for cracked samples with respect to Un-cracked

Series	Sample	Increase percentage in chloride penetration depth (d_{cl}-) (%)		
		0.05 -0.15 mm	0.15-0.25 mm	0.25-0.35 mm
Series 1 carbonated	M 0.4	55	88	112
	M 0.5	57	62	62
	M 0.6	71	71	71
Series 2 un- carbonated	M 0.4	48	83	83

	M 0.5	100	114	107
	M 0.6	71	71	72

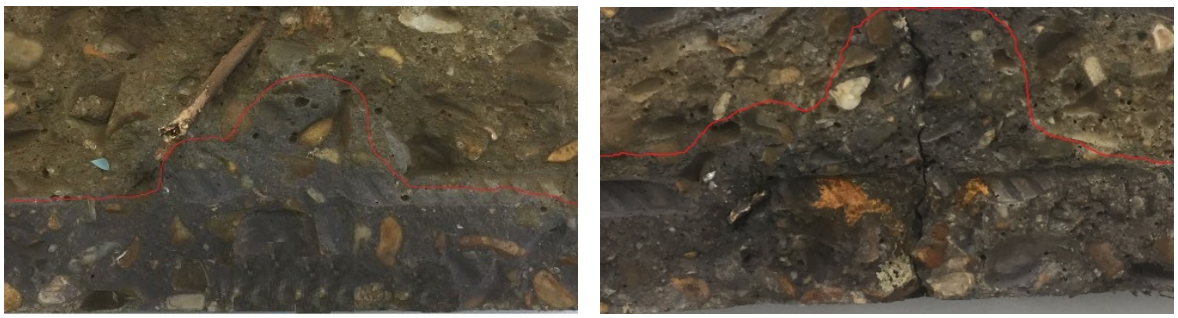

a: M 0.4-crack width 0.1 mm **b: M 0.5-crack width 0.1 mm**

Fig. 9. Effect of w/c ratio on the penetration of chloride in the cracked sample

1

2 **3.2.2 Total chloride concentration profile**

3 The total chloride concentrations for all mixes were experimentally found according to BS EN 12390- 11:2015 [25] by
4 chloride titration method for samples exposed to 15 weeks. Results for both carbonated and uncarbonated samples
5 including various crack widths and w/c ratios are presented in Fig. 10, which illustrates the changes in total chloride
6 concentration at various depth from the exposed concrete surface.

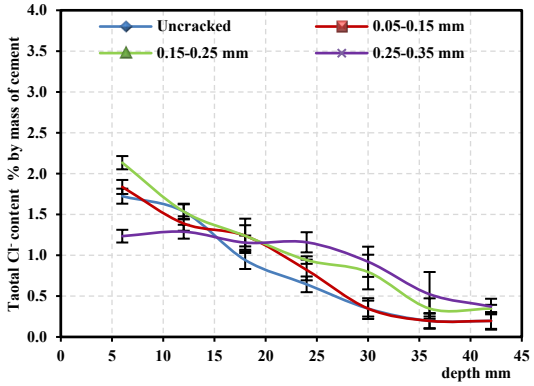

a-1: M 0.4 Un-carbonated

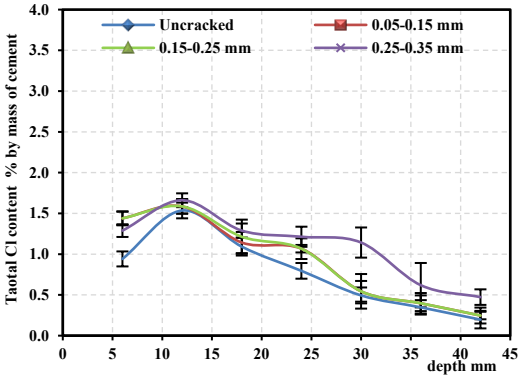

a-2: M 0.4 –carbonated

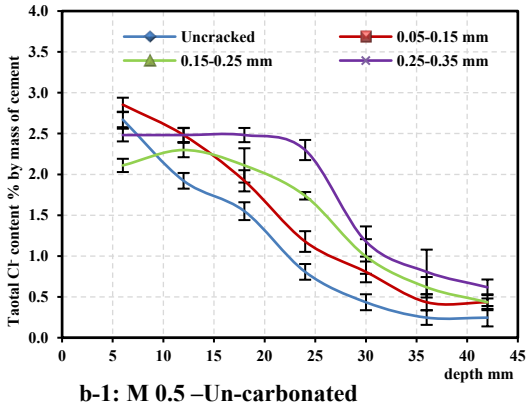

b-1: M 0.5 –Un-carbonated

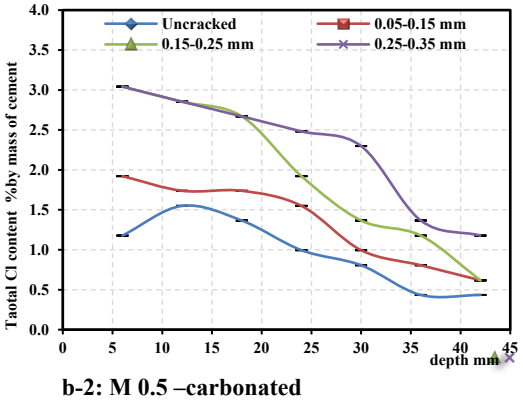

b-2: M 0.5 –carbonated

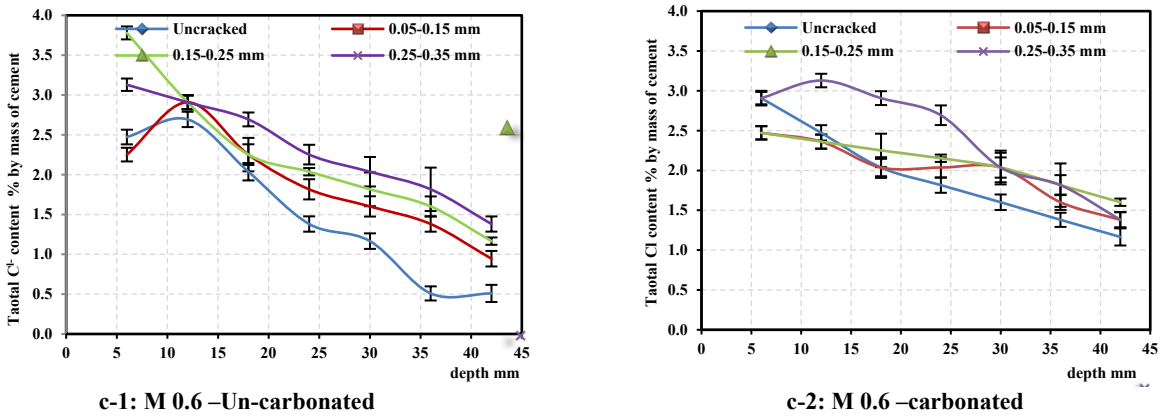

c-1: M 0.6 –Un-carbonated **c-2: M 0.6 –carbonated**

Fig. 10 The total chloride concentration profile of mixes exposing to chloride-CO_2 – chloride

The chloride concentration profiles are obtained using non-linear regression of the experimental data on the well-known model based on the Fick's second law and the key parameters are established according to BS EN 12390-11(2015) [25] (Fig.11) such as:

-The apparent diffusion coefficient, D_a.

- Surface chloride concentration, C_s.

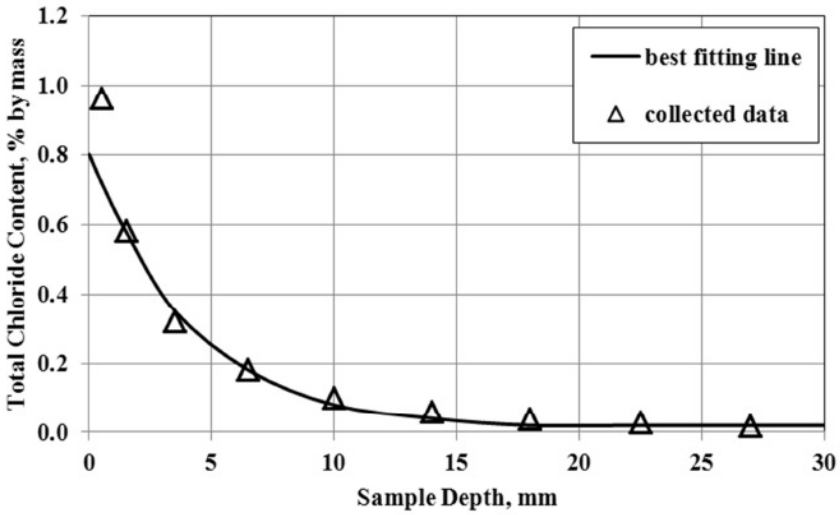

Fig.11: The chloride profile with fitted curves for surface chloride content BS EN 12390-11:2015[23]

Key observations from these results are:

(i) There is a slight increase in the chloride concentration within the carbonated samples relative to the uncarbonated samples and the difference in chloride concentration (at internal layers) in carbonated samples were higher than in uncarbonated. According to this variation in chloride concentration, the D_a and C_s values for the carbonated sample were higher than these values in the un-carbonated sample for sound and cracked samples as shown in Fig.12.

As mentioned previously, carbonation is a significant factor in reducing the pH and assists in liberating the bound chlorides within the cement and encourage to increase the chloride penetration into the concrete sample that leads to

increase the chloride concentrations (Wan et al., 2013) [5]. The bound chloride content under carbonation environment condition all approximates to zero, which shows that carbonation gives cement paste lose chloride binding capacity completely (Chang 2017) [38]

(ii): The chloride penetrates progressively further into the concrete for mixes with higher w/c ratio for (all exposure condition). In particular, higher chloride concentrations were observed near the surface of concrete due to exposure to the chloride environment. In the Fig. 12, for un-crack and almost all the cracked samples, with w/c ratio increased, apparently, the apparent chloride diffusion coefficient D_a and chloride surface concentration C_s increased significantly at the all exposure condition. It is generally accepted that the influence of increasing w/c ratio decreases chloride resistance of concrete (Dyer, 2014, Basheer et al., 2001) [3, 34]. In this study, whether increasing w/c ratio behaves the rising trend on chloride diffusion coefficient value and surface chloride concentration across all test's samples was evaluated.

There is an agreement between researchers (Neville, 2011, Dyer, 2014, Basheer et al., 2001) [1, 3, 34] that the w/c ratio of the mix and the degree of cement hydration have a significant influence on the capillary porosity of the cement paste. The degree of hydration also depends on the type of cement, however same type of cement was used throughout this study so this factor can be ignored. Thus, the increase in w/c increases the volume of capillary pores. At water/cement ratios higher than about 0.38, the volume of the gel is not sufficient to fill all the available voids so there will be some volume of capillary pores left even after the process of hydration has been completed (Neville, 2011) [1]. According to calculation details of cement hydration, the products of cement hydration in w/c ratio (0.5) may be left more capillary pores and it will increase with increase w/c ratio, such as 0.6 due to the increase of water quantity against cement. Finally, the changing in the w/c ratio has considerably affected micro-structure of the concrete by reduction in gel/space ratio and micro-structure of the concrete due to decrease in the amount of cement and increase water, these capillary pores or permeable voids are formed well path of transport for chloride into concrete deeper (Song et al., 2008) [39].

(iii): The crack width has considerably influenced the ability of chloride ions to diffuse into the concrete along the cracks for all mixes. The influence of crack varies dependent upon its width and depth that could alter the mechanism of penetration of chloride ion into the crack openings. Crack widths range from very small internal micro-cracks, to large structural cracks. The experimental data indicated that the crack width less 0.15 mm gave the highest combined effect of crack and permeability of concrete in chloride penetration for all mixes. Beyond this value (cracks $\geq$ 0.15 mm), the chlorides ion mainly penetrate through both faces of the crack opening similar to the exposed face of a concrete surface. According to chloride concentration profile, the D_a and C_s for all sample different (w/c ratio, exposure condition) increased with increase the crack width as shown in Fig.12. The impact of crack width on D_a and C_s is presented in Fig.12. In sound concrete, the transport of chloride into concrete can be occurred due to a combination of the concentration gradient, the pressure gradient and capillary sorption make the flow of chloride through permeable pores by combined transport

methods such as diffusion, permeation and capillary sorption (Basheer et al., 2001) [34]. In cracked, the new factor of transport properties in concrete are represented through permeability of concrete, which is likely to be significantly affected by the formation of cracks. The presence of cracks in concrete may influence the transport of chloride ion in concrete; they have a significant impact on diffusion and permeation of chloride ion in concrete by permeable pores. Where, the chloride diffusion coefficient in concrete may be increased according to crack width due to change of mechanism of chloride transport (Shao-feng et al., 2011, Kwon et al., 2009) [11,13]. On the other hand, the chloride concentration with penetration depth may change in same crack width due to the natural formation of cracks in the sample (width, depth, and tortuosity) or the method of measuring the diffusion coefficient of chloride. Finally, the increase the total chloride concentration with increasing crack width is the result of increasing opened exposure area to chloride solution as well as penetration through the voids or the porosity in concrete (Park et al., 2012) [12]. Fig.9 showed the influence of crack on chloride penetration throughout the crack path.

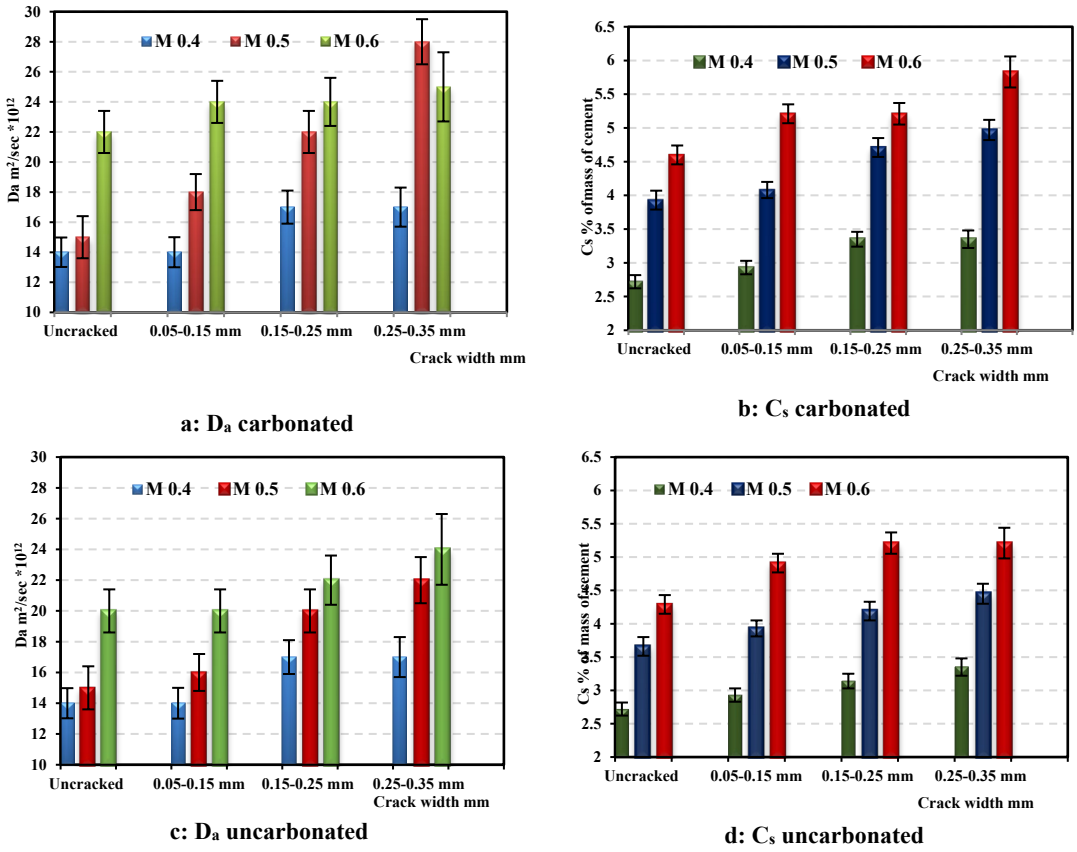

Fig. 12. Effect of w/c (M 0.4, M0.5 and M0.6) and crack width on D_a and C_s for a concrete prism with different crack width and exposure (Carbonated)

3.3 Electrochemical tests Results

The exposure of reinforced concrete samples to the chloride environment depassivates the steel in concrete and induces an electrochemical reaction. This reaction can be measured by common techniques such as half-cell potential (E_{corr}) and linear polarization resistance (LPR) in order to determine the active or passive state of the corrosion process, and the rate of corrosion. The electrochemical tests (half -cell and LPR) were carried out every 2-3 weeks during and after the exposure period.

3.3.1 Half-cell potential (E_{corr}) results

The half-cell potential measured at various intervals during the exposure of samples to chloride fog is presented in Fig. 13. ASTM C876-2015 [32] provides useful interpretation of these results. Half-cell potential values of higher than −126 mV measured with reference to the saturated calomel electrode (SCE) refers to more than 90% probability of inactive corrosion (passive state). The potential values in the range of −126 to −276 mV SCE represents intermediate corrosion risk. Whereas, the potential values more negative than −276 mV SCE represents a greater than 90% probability of active corrosion (Song and Saraswathy, 2007, Bertolini et al., 2013) [40,41].

(i) Fig. 13-a, b and c presents the results of specimens (exposure to chloride fog without carbonation) for the three mix designs used in this study. An increase in exposure time of samples to chloride fog monotonically increases the more negative values of the electrode potential, i.e. the probability of corrosion increases with the duration of exposure. The electrode potential for many samples had exceeded the threshold potential (-126mV SCE) between the passive to intermediate corrosion risk condition after 40 days of exposure. The specimens M 0.5 and M 0.6 attained the potential values that are more negative than -276 mV SCE after 80 days of exposure for all samples.

(ii) Fig. 13-d, e and f presents the results of carbonated samples for the three mixes used in this study. The exposure of samples to the CO_2 environment has a considerable impact on the electrode potential of steel reinforcement. A step change in potential drop can be seen at around 80 days in all carbonated samples (during the period of CO_2 exposure), whereas the potential values for samples M 0.4 remained more positive than -126 mV SCE (> 90% probability of no corrosion) for the uncarbonated samples. This suggests that the corrosion conditions have been altered (from passive to active corrosion state) for this concrete mix due to the presence of carbonation.

(iii) The negative values of half-cell potential generally increased with the increase in w/c of concrete (i.e. between M0.4, M0.5 and M0.6 concrete mixes) for both uncarbonated and carbonated specimens. Table 6 details which samples had exceeded the threshold value of more negative than -276mV (>90% probability of active corrosion), and their respective exposure duration when the threshold was reached.

(iv) The cracks within the samples increases the transport of chloride, accelerating the transition of corrosion from passive to active state. This can be seen from Fig. 13 where the electrode potential value generally negative shifted with the increase in crack width. Hence, the probability of corrosion is proportional to the crack width. For carbonated samples, the impact of crack opening on the potential drop was not clear since samples changed from passive to active corrosion condition during CO_2 exposure phase.

Considering a drastic change in the half-cell potential leading to values more negative than −276 mV (SCE) (Song and Saraswathy, 2007) [40], it was possible to assess the transition from passive to active corrosion in M 0.5 and M 0.6 specimens by a chloride concentration higher than 1% for total chloride or free chloride higher than 0.3% (Bouteiller et al., 2012, Angst, et al. 2009, Tuutti, 1982) [33, 42,43] as shown in Fig.10. However, these results will be explained in further detail in the next section when these results are compared with the LPR results and determine the rate of corrosion in these specimen.

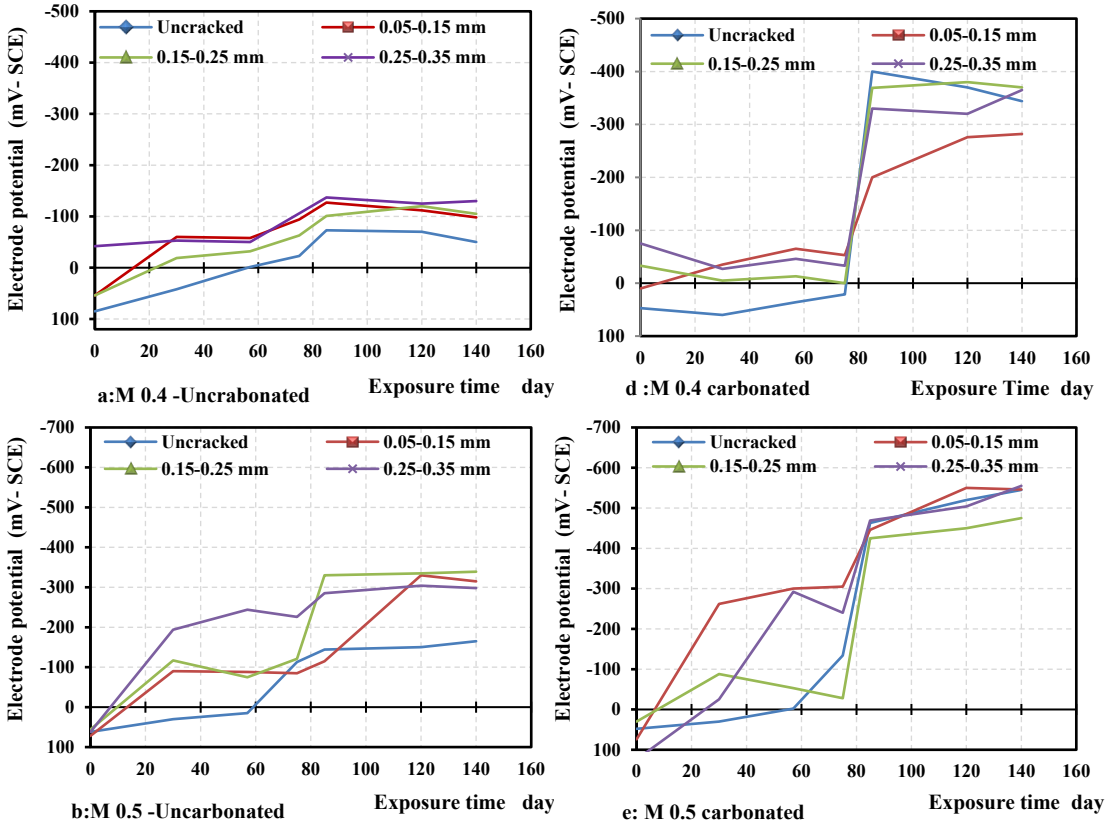

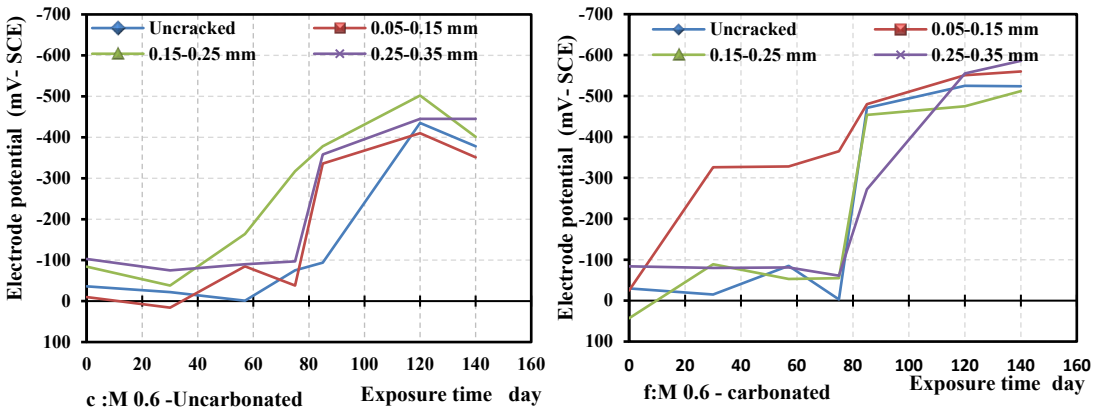

Fig. 13. Effect of w/c and carbonation on half-cell potential of reinforced concrete samples (a,b and c) uncarbonated samples and (d,e and f) carbonated samples

Table 6 Summary of half – cell potential less than -276 mV and the age

Series	Sample	Un-cracked		0.05-0.15 mm		0.15-0.25 mm		0.25-0.35 mm	
		E_{corr} ≤-276	Age*	E_{corr} ≤-276	Age*	E_{corr} ≤-276	Age*	E_{corr} ≤-276	Age*
Series1 carbonated	M 0.4	Y	85	Y	85	Y	85	Y	85
	M 0.5	Y	85	Y	85	Y	85	Y	85
	M 0.6	Y	85	Y	30	Y	85	Y	75
Series 2 uncarbonated	M 0.4	-	-	-	-	-	-	-	-
	M 0.5	-	-	Y	120	Y	85	Y	85
	M 0.6	Y	110	Y	85	Y	75	Y	80

E_{corr}: Half-cell potential is more negative than -276 mV, high probability that corrosion is occurring.
* Age: Time of arrival half-cell potential-SCE is ≤ -276 mV.
Y: Yes, E_{corr} ≤ -276 mV.

3.3.2 Linear Polarization Resistance results

Polarization resistance (Rp) of steel in concrete mixes, determined by the linear polarization resistance (LPR) technique, were tested at different ages of exposure to the chloride environment. The corrosion current density (i_{corr} in $\mu A/cm^2$) is found using Stern-Geary Equation ($i_{corr}=B/Rp$) for the reinforcement concrete sample (Katwan, 1988) [44]. B is constant, it is commonly considered equal to 26 mV for active corrosion and 52 mV for the passive state (Andrade and González, 1978) [45]. The focus of the current study is the rate of corrosion, i.e. the corrosion will be in active state. Therefore, value of B was selected as 26mV for the results below (Bouteiller et al., 2012) [33].

Considering the RILEM (TC 154-EMC) (Andrade et al., 1990, Andrade and Alonso, 2004) [46,47] recommendations, four corrosion levels expressed in terms of the corrosion current densities i_{corr}, as shown in Table 7, are useful for the interpretation of these results. The corrosion rate used for the discussion purposes in the following section will be the moderate to high corrosion, i.e. i_{corr} greater than 0.5 $\mu A/cm^2$, which is shown using symbol M in Table 8 below.

Table 7 Corrosion current vs. condition of the rebar (Andrade et al., 1990) [47]

Corrosion current density (i_{corr})	The condition of the rebar
$i_{corr} < 0.1\ \mu A/cm^2$	Passive condition
i_{corr} 0.1 - 0.5 $\mu A/cm^2$	Low to moderate corrosion
i_{corr} 0.5 - 1.0 $\mu A/cm^2$	Moderate to high corrosion
$i_{corr} > 1.0\ \mu A/cm^2$	High corrosion rate

The evolution of corrosion current densities for all concrete specimens exposed to chloride ingress and CO_2 conditioning are presented in Fig.14 and Table 8.

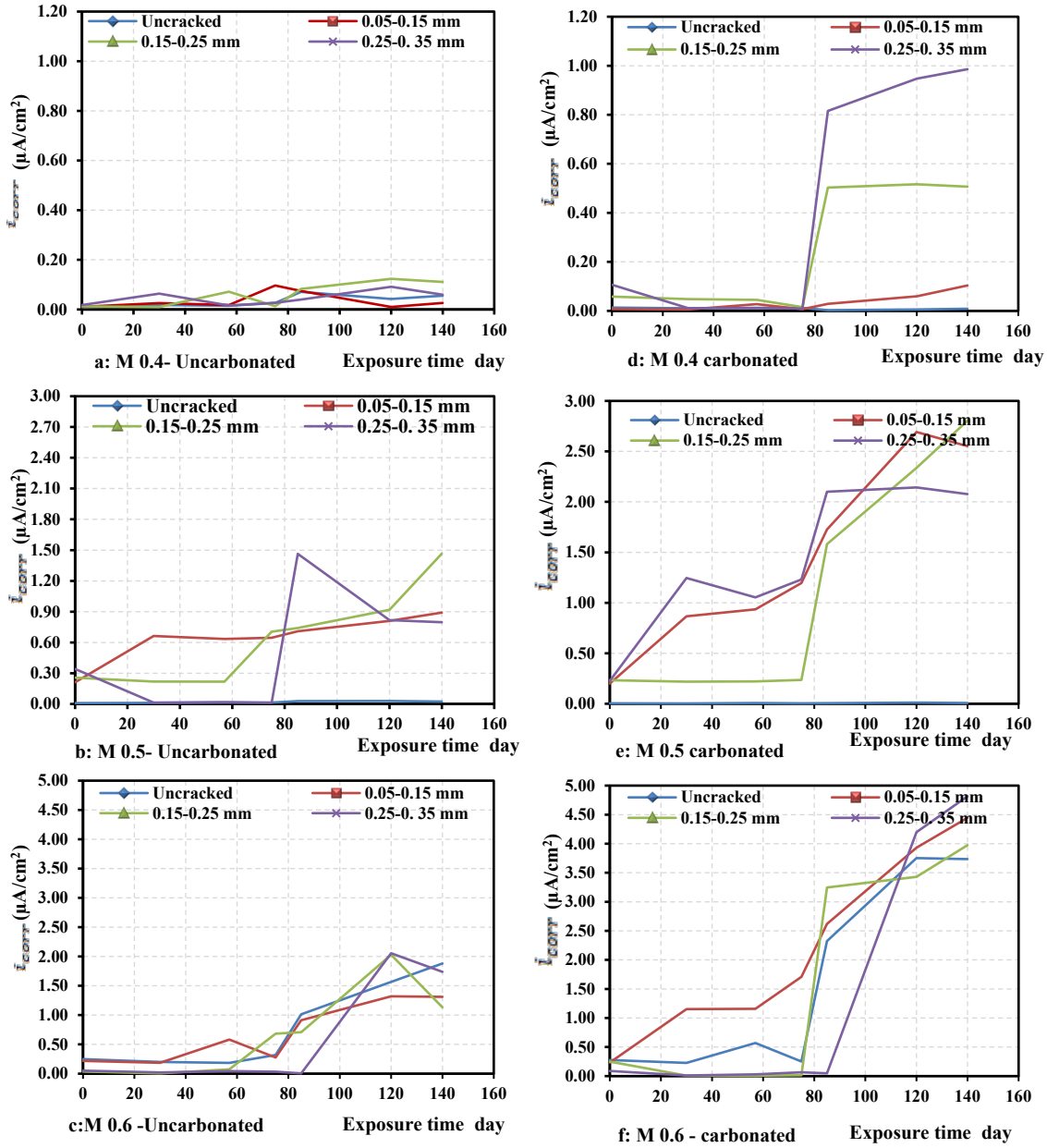

Fig.14. Effect of w/c and carbonation on corrosion current density of reinforced concrete prisms

Table 8 Summary of i_{corr} higher than 0.5 µ A/cm² and the age of arrival this level

Series	Sample	Un-cracked		0.05-0.15 mm		0.15-0.25 mm		0.25-0.35 mm	
		i_{corr} ≥ 0.5	Age* day	i_{corr} ≥ 0.5	Age* day	i_{corr} ≥ 0.5	Age* day	i_{corr} ≥ 0.5	Age* day
Series 1 carbonated	M 0.4	-	-	-	-	-	-	M	85
	M 0.5	-	-	M	30	M	85	M	30
	M 0.6	M	85	M	30	M	85	M	85
Series 2 Un- carbonated	M 0.4	-	-	-	-	-	-	-	-
	M 0.5	-	-	M	30	M	75	M	85
	M 0.6	M	85	M	85	M	75	M	85

Corrosion current (i_{corr})higher than 0.5 µ A/cm², the corrosion is occurring with range moderate to high.

*Age: Time of arrival i_{corr} higher than 0.5 µ A/cm².

M: Moderate to high corrosion rate.

Some observations from these results are;

(i): The carbonation has a significant impact on i_{corr} of steel reinforcement. (ii): The i_{corr} values increased progressively as the time of exposure to chloride fog increased. (iii): Generally, the i_{corr} increases with the increase in the w/c of concrete. (iv): The value of i_{corr} increases with the increase in crack size, which can be clinked to the increased transport of chloride ions into the cracked concrete.

The corrosion current density increases over time as the exposure progresses and these were different for specimen depending upon other conditions such as exposure (or not) to carbonation, w/c ratio and crack width. The results depict that most specimen had exceeded the recommended corrosion current density for passive state (0.1 μ A /cm^2) after 20 days of exposure to chloride environment. After this time, the i_{corr} mostly fall within the Low to moderate corrosion range but in many cases falls within the band of moderate to high corrosion (i_{corr} are more than 0.5 μ A /cm^2) after 60 days of exposure in samples M 0.5 and M 0.6. Whilst for carbonated samples, the i_{corr} increased sharply again at 80 days as shown in Fig.14, beyond exposed to CO_2 environment condition. On the other hand, i_{corr} values for the rebar in M 0.4-uncracked and carbonated samples remained passive (less 0.1 μ A /cm^2) during the overall period of the chloride exposure. While, the i_{corr} of samples of (M0.4-crack width greater than 0.15 mm – Series1) increased suddenly after exposed to CO_2 due to increasing DoC as shown in Fig.5.

The results also demonstrate that an increase in w/c ratio of reinforced concrete accelerated the corrosion current density, i_{corr} of reinforcement and the samples became within considerable risk of corrosion range. The corrosion rate values for almost all M 0.4 carbonated samples remained in the range of passive corrosion condition, i.e. the threshold chlorides did not reach adequate depths to initiate breaking down of the passive layer of steel rebar as shown in as shown in Fig. 14-a. Conversely, for rebar in the relatively porous concrete specimens (M 0.6-Un-cracked) a significant increase of i_{corr} was observed over time. After the few wetting-drying cycles, i_{corr} values of the specimens were higher than 0.5 μA/cm^2 (i.e. within active corrosion state). A drastic i_{corr} increase was observed after week 10 for specimen's Series 1and 2, leading to values that falls within the range of the higher corrosion rate. These can be attributed to the penetration of chlorides beyond the rebar level (in accordance with the chloride determinations at as shown in Fig. 10(c-1 and c-2). Table 8 is listed all the cases have i_{corr} more than 0.5 μA/cm^2 and the time of arrival this corrosion rate.

As shown previously in chloride concentration section (3.2.2), the factors affecting chloride concentration were carbonation, w/c and crack width. These factors have a significant role in the progression of corrosion rate by increasing the chloride concentration. In carbonated samples, the presence of a small chloride in carbonated concrete accelerates the corrosion rate due to reduction of the pH in pore water in concrete that lead to changing the environment of the concrete's micro- structures (Neville, 2011)[1]. Additionally, reinforced concrete structures are more vulnerable to corrosion by the combined impact of chloride and carbonation than those with only one of the two sources (Broomfield, 2007) [4]. The

carbonation in concrete structures is the onset of chemical and physical processes toward the deterioration of concrete structures and appropriate environment to activate the chloride role in the initiation stage of the reinforcement in concrete structures.

In un-cracked concrete, the transport of chloride ions into concrete is governed by different processes (i.e. diffusion, permeation and capillary sorption) (Basheer et al., 2001) [34] and the transport properties of concrete are mainly depended on the porosity of concrete and formation of a crack. The w/c ratio and type of binder can mainly affect the porosity, preamble voids and the path of transport for chloride into concrete (Song et al., 2008) [39]. Where, the chloride penetration resistance of concrete decreases with the increase in w/c ratio that leads to an increase in the electrochemical reaction, (initiation and propagation of corrosion) (Bouteiller et al., 2012) [33]. The corrosion onset for M 0.6 specimens has higher porosity as observed in section 3.1, was highlighted from a potential drop, E_{corr} (Fig. 13- c and f) together with an increase of corrosion rate (Fig. 14- c and f) after few weeks depending on exposure condition. Whilst, the less porous M 0.4-uncracked specimens did not corrode significantly during the 16 weeks of chloride wetting-drying cycling as half-cell potential values remained in the uncertain corrosion range (Fig.13-a) and as corrosion currents were lower than 0. 1 $\mu A/cm^2$. Moreover, from visual examination of the steel rebars after 16 weeks, M 0.6 (carbonated and uncarbonated) specimen showed a corroded surface as shown in Fig. 15 while in M 0.4 specimen only a black rust area was seen. Finally, the increase w/c ratio achieves the decrease in the concrete quality by increasing the porosity and water absorption as well as a decrease in the strength, and at final, the decreasing concrete quality gives increases in the corrosion rate (Otieno et al., 2008) [48].

On the other hand, the presence of cracks in concrete may negatively influence the significant parameters of transport of chloride ion, Cl^-, and carbonic ion $CO3^{-2}$, in reinforced concrete and hence the chloride ingress rate, thereby influencing reinforcement corrosion process (Jacobsen et al., 1996) [49]. The cracks provides a preferential channels for the diffusivity of potentially aggressive agents such as chloride ions, Cl^-. They have a significant impact on the diffusion and permeation of aggressive species in concrete. Many studies (Francois and Arliguie, 1991, Jang et al., 2011,Van den Heede et al., 2014,) [50-52] concluded that chlorides penetrate rapidly through cracks and accelerate chloride-induced corrosion by increasing concrete penetrability as shown in Fig.7 and 10.

The time required to initiate corrosion is shorter for one with the wider crack (Berke et al., 2014, Park et al.2012) [12, 53]. In general, the corrosion rate increases with increasing crack width but is sensitive to concrete quality (Otieno et al., 2008) [48]. This is the general idea of the effect the crack on corrosion rate, however, the crack width has the different performance of corrosion rate. In small crack width, the corrosion products due to the first corrosion process affects the

penetration of chloride by filling the end of crack opening and sometimes the cement materials may be self-healing of the crack by new hydration products later (Van den Heede et al., 2014Ismail et al., 2008,) [52,54].

a: M 0.6 -cracked 0.25 mm (Carbonated) **b: M 0.6 -cracked 0.25 mm (Uncarbonated)**

Fig. 15. Effect the carbonation and chloride cocentration on the corrosion of steel bar in concrete

4 Conclusion

This study explores the impact of carbonation on the chloride penetration, and rate of corrosion in concrete samples cracked by service loading. Chloride penetration, carbonation depth and corrosion were investigated by using an accelerated environment test programme for (Cl^- and CO_2). The depth of carbonation, DoC was measured using phenolphthalein indicator, whereas chloride depth front (d_{cl^-}) and chloride content were determined by $AgNO_3$ spraying and titration with (0.1M $AgNO_3$) respectively. The electrode half- cell potential and LPR were employed to establish the corrosion condition and rate respectively. DoC using phenolphthalein indicator and pH investigations made it possible to develop better understanding of the impact of carbonation on chloride penetration, half-cell corrosion potential (corrosion activity) and LPR (corrosion rate). The following conclusions can be drawn from the results;

1- The quality of concrete, i.e. w/c ratio, porosity, and compressive strength affects the depth of carbonation and chloride penetration depths.
2- The chloride penetration significantly increases within the concrete samples exposed to CO_2 environment for all mixes used in the study.
3- The half-cell corrosion potential is significantly higher in carbonated samples when exposed to the chloride environment and progressively increases with the exposure time.
4- For concrete specimens exposed to carbonation and chlorides, crack widths influence the corrosion activity and therefore, should be considered in service life prediction models.

5- In the carbonated samples, the electrode half-cell potential and corrosion rate increase sharply with the increase in chloride exposure with the progress of the age.

6- The carbonation and cracks accelerate chloride-induced corrosion by increasing concrete penetrability. In general, the corrosion rate increases with increasing crack width but is also sensitive to the concrete quality.

7- The use of LPR measurements to monitor corrosion in cracked concrete was found to be well matched with half-cell potential measurements.

8- Chloride penetration in the vicinity of the cracks is considerably higher due to relatively faster penetration of Cl^- into the crack followed by orthogonal outward diffusion into the un-cracked concrete surrounding the crack.

References

1. Neville, A.M., 2011. Properties of concrete. (Five and Truly Final Edition) London: Pearson Education Limited.
2. Hussain, S., Rasheeduzzafar, Al-Mu&am, A. and Al-Gahtani, A., Factors affecting threshold chloride for reinforcement in concrete. Cement and Concrete Research, 25(7) (1995) pp. 1543-1555.
3. Dyer, A., Concrete durability. New York: 2014. Taylor& Francis Group, LLC.
4. Broomfield, J.P. Corrosion of steel in concrete.2nd edition .London.Taylor &Francis (2007).
5. Wan,X., WttmannI,F. ,Zhao,T. and Fan,H., 2013. Chloride content and pH value in the pore solution of concrete under carbonation. Journal of Zhejiang University-Science A (Applied Physics & Engineering), 14(1),(2013) pp71-78.
6. Geng, J., D. Easterbrook, Q.-F. Liu and L.-Y. Li .Effect of carbonation on release of bound chlorides in chloride-contaminated concrete. Magazine of Concrete Research 68(7)(2016): 353-363. 7.Shen, X.-h., Q.-f. Liu, Z.
7. Hu, W.-q. Jiang, X. Lin, D. Hou and P. Hao. Combine ingress of chloride and carbonation in marine-exposed concrete under unsaturated environment: A numerical study. Ocean Engineering 189(2019); 106350.
8. American Concrete Institute, ACI Committee 224. R, 01. Control of Cracking in Concrete Structures. (2001) Farmington Hills, Mich.: ACI.
9. Concrete Society. Non-structural cracks in concrete, TR **22** (2010) Concrete Society.
10. Morcous, G. and Louis, Z. Maintenance Optimization of Infrastructure Networks using Genetic Algorithms, Journal of Automation in Construction, **14** (1), 2005, pp 129–142.
11. Sheo-Feng, Z., Chun-Hua, L. and Rong-Gui, L, Experimental determination of chloride penetration in cracked concrete beams. 2011 international conference on advanced in engineering, proceeding 24, (2011) pp 380-384.
12. . Park, S., Kwon, S., and Jung, S., Analysis technique for chloride penetration in cracked concrete using equivalent diffusion and permeation. Construction and Building Materials, **29**, (2012) pp. 183–192.

13. Kwon S., Na U., Park S.and Jung S., Service life prediction of concrete wharves with early-aged crack: a Probabilistic approach for chloride diffusion. Structural Safety, **31**, (2009) pp. 75–83.
14. Neville, A.M., Brooks, J.J., Concrete Technology. (Second Edition) London: 2010. Pearson Education Limited.
15. BS EN 197-part 1: 2011. Cement-part 1: Composition, specifications and conformity criteria for common cements.
16. BS.882 /1983.Aggregate from natural sources for concrete. British Standard Institution.
17. BS 4449:2005+A3:2016. Steel for the reinforcement of concrete. Weldable reinforcing steel. Bar, coil and decoiled product.
18. Teychenné, D.C., E Franklin, R.E. and Erntroy, H. C., Design of normal concrete mixes. Second edition. Building Research Establishment. Garston, Watford,(1988).
19. BS EN 12390 part- 2:2009. Testing hardened concrete –;Part 2: Making and curing specimens for strength tests.
20. Bungey, J.H. , Millards, S.G., and Grantham, M.G.. Testing of concrete in structures.Fourth edition, Abingdon, 2006, Taylor & Francis e-Library, pp.79-80.
21. ASTM C642:2013, Density, Absorption, and Voids in Hardened Concrete.
22. BS EN 12390, part 3:2000. Testing hardened Concrete Part 3: Compressive strength of test specimens.
23. Yuan.Q. , Shi, C., He, F. Schutter, G. Audenaert, K., and Zheng, K., Effect of hydroxyl ions on chloride penetration depth measurement using the colourimetric method. Cement and Concrete Research Vol.38, (2008) pp.1177–1180.
24. He, F., Shi ,C., Yuan, Q., An, X. and Tong, B. Calculation of chloride concentration at color change boundary of AgNO3 colorimetric measurement. Cement and Concrete Research **41** (2011) pp.1095–1103.
25. BS EN 12390, Part 11:2015, Testing hardened concrete: Determination of the chloride resistance of concrete, unidirectional diffusion.
26. AL-Amoudi, O., Rasheeduzzafar and Maslehuddin, M. Carbonation and corrosion of rebars in salt contaminated OPC/PFA concretes. Cement and Concrete Research, **21**(1991),pp. 38-50.
27. BS EN13295:2004. Products and systems for the protection and repair of concrete structures — Test methods — Determination of resistance to carbonation.
28. BS EN 12390-10:2018. Testing hardened concrete. Determination of the e carbonation resistance of concrete at atmospheric level of Carbone dioxide, European Committee for Standardization.
29. Mc Polin, D., Basheer, M., Long, E., Grattan, V. and Sun , T. New Test Method to Obtain pH Profiles due to Carbonation of Concretes Containing supplementary Cementitious Materials, journal of materials in civil engineering , ASCE, **19** November (2007), pp. 936-946.

30. Wang, J., Basheer ,M., Nanukuttan, S., Long ,A., Bai, Y. Influence of service loading and the resulting micro-cracks on chloride resistance of concrete. Construction and Building Materials,Vol. **108** (2016) pp. 56–66.
31. BS EN ISO 10523:2012. Water quality — Determination of pH.
32. ASTM C 876:2015, Half-Cell Potentials of Uncoated Reinforcing Steel in Concrete.
33. Bouteiller, V., C. Cremona, V. Baroghel-Bouny.. Corrosion initiation of reinforced concretes based on Portland or GGBS cements: Chloride contents and electrochemical characterizations versus time. Cement and Concrete Research 42(11), (2012) pp.1456-1467.
34. Basheer, L., J. Kropp and D. J. Cleland. Assessment of the durability of concrete from its permeation properties: a review. Construction and building materials 15(2-3), (2001) pp. 93-103.
35. Chi, J. M., Huang, R.and Yanlg, C. C. Effect of Carbonation on Mechanical Properties and Durability of Concrete Using Accelerating Testing Method. ; Journal of Marine Science and Technology, 10(1),(2002) pp. 14-20.
36. Audenaert, K., G. De Schutter and L. Marsavina. Influence of cracks and crack width on penetration depth of chlorides in concrete. European journal of environmental and civil engineering 13(5), (2009) pp. 561-572.
37. Suzuki, K., Ohno, Y., Praparntanatorn, S. and Tamura, H., . Mechanism of Steel Corrosion in Cracked Concrete, Corrosion of Reinforcement in Concrete, Ed. Page, C., Treadaway, K. and Bramforth, P., London: Society of Chemical Industry, (1990) pp. 19–28.
38. Chang, H.. Chloride binding capacity of pastes influenced by carbonation under three conditions. Cement and Concrete Composites 84(2017) pp.1-9.
39. Song, H.,Lee,C.and Ann,K.,Factors influencing chloride transport in concrete structures exposed to marine enlivenments. Cement and concrete composite , **30** , (2008) pp.113-121.
40. Song, H.W and Saraswathy,V. Corrosion Monitoring of Reinforced Concrete Structures - A Review, International Journal of Electro chemistry Science , 2(2007) pp. 1-28.
41. Bertolini, L., B. Elsener, P. Pedeferri, E. Redaelli and R. B. Polder (2013). Corrosion of steel in concrete: prevention, diagnosis, repair, John Wiley & Sons.
42. Angst, U., B. Elsener, C. K. Larsen and Ø. Vennesland (2009). "Critical chloride content in reinforced concrete—A review." Cement and concrete research 39(12) pp. 1122-1138.
43. Tuutti, K.Corrosion of steel in concrete. Swedish cement and concrete research institute (1982).
44. Katwan, M.1988.Corrosion fatigue of reinforced concrete. Ph.D., Thesis. University of Glasgow.
45. Andrade, C. and J. González. Quantitative measurements of corrosion rate of reinforcing steels embedded in concrete using polarization resistance measurements. Materials and Corrosion **29**(8), (1978) pp. 515-519.

46. Andrade, C. and C. Alonso. Test methods for on-site corrosion rate measurement of steel reinforcement in concrete by means of the polarization resistance method. Materials and Structures **37**(9),(2004) pp. 623-643.

47. Andrade, C., M. C. Alonso and J. A. Gonzalez. An initial effort to use the corrosion rate measurements for estimating rebar durability. Corrosion rates of steel in concrete, ASTM International.(1990).

48. Otieno, M., M. Alexander and H. Beushausen . Corrosion propagation in cracked and uncracked concrete. Concrete Repair, Rehabilitation and Retrofitting II: 2nd International Conference on Concrete Repair, Rehabilitation and Retrofitting, ICCRRR-2, 24-26 November (2008), Cape Town, South Africa, CRC Press.

49. Jacobsen, S., J. Marchand and L. Boisvert (1996). Effect of cracking and healing on chloride transport in OPC concrete. Cement and Concrete Research 26(6),pp. 869-881.

50. Francois, R. and G. Arliguie. Reinforced concrete: correlation between cracking and corrosion. Special Publication 126, (1991) pp. 1221-1238.

51. Jang, S. Y., B. S. Kim and B. H. Oh. Effect of crack width on chloride diffusion coefficients of concrete by steady-state migration tests. Cement and Concrete Research 41(1), (2011) pp. 9-19.

52. Van den Heede, P., M. Maes and N. De Belie . Influence of active crack width control on the chloride penetration resistance and global warming potential of slabs made with fly ash+ silica fume concrete. Construction and Building Materials 67, (2014) pp.74-80.

53. Berke, N., A. Bentur and S. Diamond. Steel corrosion in concrete: fundamentals and civil engineering practice, CRC Press(2014).

54. Ismail, M., A. Toumi, R. François and R. Gagné. Effect of crack opening on the local diffusion of chloride in cracked mortar samples." Cement and concrete research 38(8-9)(2008) pp. 1106-1111.